

Performance of Dual-Hop Forward Relay Diversity Systems in Wireless Nakagami Fading Channels

F.Sahul Hameed, A.Mohamed Mian and P.Mohamed Fathima

Abstract- Future wireless communication systems have to support very high data rates in order to achieve any-time, anywhere, all-service connectivity. The vision is not feasible with the conventional cellular architecture as it demands a drastic increase in the number of base stations. Introduction of wireless relays is one possible solution to the problem to increase the capacity as well as radio coverage area with minimal increment in the capital expenditures. In this paper we find the end-to-end statistics of a two hop non-regenerative relay branch, each hop being Nakagami- m faded. Closed form expressions for the probability density functions of the signal envelope at the output of a selection combiner and a maximal ratio combiner at the destination node are also derived and analytical formulations are verified through computer simulation. These density functions are useful in evaluating the system performance in terms of bit error rate and outage probability.

Keywords—co-operative diversity, diversity combining, maximal ratio combining, selection combining.

I. INTRODUCTION

In recent years, the rapid expansion of wireless communications has put a significant pressure to the current wireless network infrastructure to cope with demands for higher throughput, higher robustness and better coverage. It is expected that such demands would even be stronger in the future fourth-generation (4G) wireless networks. No longer limited to a medium for only voice transmission, wireless communications have assumed an important role in transmitting data at higher rates and streaming multimedia services, such as video, at higher quality of service (QoS) requirements.

This demand directly conflicts with the properties of the wireless medium. In a wireless transmission the signal quality suffers severely from a bad channel quality due to fading caused by multi-path propagation. Basically, fading in a wireless channel refers to the time and frequency variations of the channel quality. To reduce such effects, diversity can be used to transfer the different samples of the same signal over independent channels realized in time, frequency, polarization or over space. In this paper, diversity is realized by using a third station as a relay and the source/transmitter and the destination/receiver being the other two. Dual-hop relaying is a promising technique to achieve broader coverage and to mitigate wireless channel impairments.

The main idea of cooperative diversity schemes is to use relay nodes as virtual antennas to facilitate the communication of a source destination pair. Potential application areas of cooperative diversity include advanced cellular architectures, mobile wireless ad-hoc networks, and other hybrid networks in order to increase coverage, throughput, and capacity to transmit to the actual destination or next relay.

The relays of a cooperative diversity system can be broadly classified into two different categories depending on their functionalities. The relays are classified as either non-regenerative or regenerative type. The non-regenerative relays simply amplifies and forwards (A & F) the received signal to the next participating relay and/or the destination node. The complexity and latency of these type of relays are less as compared to the regenerative type. A regenerative relay decodes, encodes and then forwards the received signal to the next participating relay and/or the destination node. As the received signal requires to be decoded and encoded at the relay, the process proves to be computationally complex and time intensive.

The non regenerative relays are generally preferred when complexity and/or latency issues are important as these relays are usual battery powered and has limited processing capacities [3]. However, in a non-regenerative system, because of the presence of intermediate relay nodes, the statistics of the signal received at the destination depends on the channel conditions the signal experiences in the individual links. For properly utilizing the characteristics of a relay link in system design we require to understand the statistical behavior of such channels. Analysis of statistical behavior of relay channel has been a research area of considerable interest and recently some papers dealing with the methods of determining the statistics of such relay channels have appeared in the literature [3][5].

Mostly the individual relay links are assumed to be independent Rayleigh faded channels. In this communication we consider two-hop relay links, the individual links to be independent and but not necessarily identical Nakagami- m distributed but not necessarily identical. The Nakagami fading model is considered because of its flexibility of changing the individual link statistics by changing the parameter m . The rest of the paper is organized as follows: In section 2 we discuss a two hop relay system. Section 3 deals with the diversity combining techniques, with reference to selection and maximal ratio combining in a relay based system. The simulation results are presented in

F.Sahul Hameed, A.Mohamed Mian and P.Mohamed Fathima are working as Asst.Prof of ECE Dept, C.Abdul Hakeem College of Engg&Tech, Tamil Nadu, India, Emails: pmd_fathi2005@yahoo.co.in, bfjsahul@rediffmail.com, ammian79@rediffmail.com

section 4. Finally in section 5, we make the concluding remarks of the paper.

II. TWO HOP RELAY BASED SYSTEM

The simplest form of relay based communication is a two-hop communication link as shown in Fig. 1. The first hop is from the source node to the relay and the second is from the relay to the destination node. The source node may be a base station in case of advanced cellular architectures or a mobile station in a ad-hoc network.

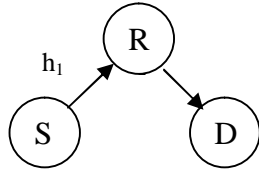


Fig. 1. A typical two hop relay based system.

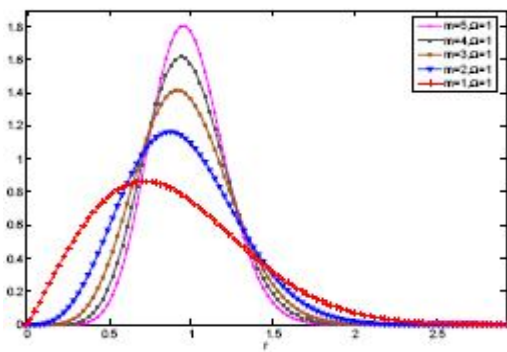


Fig. 2. The plot of Nakagami-m distribution for different values of m.

In the rest of the paper we assume the relay to be an ideal noise free repeater of non-regenerative type. Relays of non-regenerative types may be further classified into two different groups based on the type of amplification. A relay with constant amplification factor is said to be a fixed gain relay. For a variable gain relay, the amplification factor varies with time. For most cases, the variation depends on the variation of the channel. In our discussion we consider the relays to be of fixed gain type. The gain is assumed to be unity without any loss of generality. Assumption of noise free repeater simplifies analytical modeling. Subsequently, through simulation studies we estimate the maximum signal to noise ratio level at the relay at which the system bit error rate performance is not degraded exceeding a specified root mean square (RMS) error level. In Fig. 1. the signal reaches the destination (D) from the source (S) via a relay node (R). $h_1(t)$ and $h_2(t)$ represent the channel between the S-R and R-D link respectively. As mentioned, $h_1(t)$ and $h_2(t)$ are modeled as Nakagami-m distributed so that various fading scenarios can be generated as particular cases of the generalized model. The probability density function (pdf) of the amplitudes of $h_1(t)$ and $h_2(t)$ may be written as [4]

$$\int H_i(H_i) = 2 \left(\frac{m_i}{\Omega_i}\right)^{m_i} \frac{h_i^{2m_i-2}}{\Gamma(m_i)} \exp\left(-\frac{m_i}{\Omega_i} h_i^2\right) \quad (1)$$

where, $m_i > 1$ and $i=1,2$. $\Gamma(\cdot)$ represents the Gamma function. m_i denotes the m parameter of Nakagami-m distribution for the i^{th} hop. For $m=1$, we get the conventional Rayleigh fading model while by taking $m > 1$, the channel is

made to behave more like a Rician channel. Fig. 2. shows the plot of Nakagami distribution for different values of m .

H_1 and H_2 are the random variables (RVs) representing the amplitudes of the links S-R and R-D respectively. m_1 and m_2 are the corresponding Nakagami-m parameters. In a typical 2-hop cooperative relaying environment, the source transmits the information in a time slot $T/2$ and the relay amplifies and retransmits the same information to the destination node in the next $T/2$ time slot. For the flat fading case the received signal at the destination node may be written as,

$$y(t) = A(t) h_1(t) h_2(t) x(t) + A(t) h_2(t) n_1(t) + n_2(t) \quad (2)$$

for,

$$\frac{T}{2} \leq t \leq T$$

where,

$x(t)$ is the transmitted signal.

$A(t)$ is the gain of the relay.

$n_1(t)$ and $n_2(t)$ are the additive noise at the relay and the destination respectively.

As mentioned, for the sake of simplicity but without any loss of generality the relay is assumed to be a constant gain relay having an unity gain, i.e. $A(t)=1$. Moreover the relay is assumed to behave like a noise free repeater, thus $n_1(t)=0$. So (2) may be rewritten as,

$$y(t) = h_1(t) h_2(t) x(t) + n_2(t) \quad (3)$$

The effective channel between the source and the destination is basically the product of two Nakagami-m distributed RVs and can be written as $Z = H_1 H_2$. The density function of the RV Z gives the channel statistics between the source and the destination via a relay. The density function of any RV obtained from the product of two independent RVs is shown in [10].

$$f_z(z) = \int_{-\infty}^{\infty} f_{H_1}(h_1) f_{H_2}\left(\frac{z}{h_1}\right) \frac{1}{|h_1|} dh_1 \quad (4)$$

where, f_{H_1} and f_{H_2} are the probability density functions of the independent random variables H_1 and H_2 respectively. As f_{H_1} and f_{H_2} are zero for $h_1 < 0$, hence the lower limit of (4) may be set to zero. From (1) and (4) we obtain,

$$f_z(z) = \frac{4}{z \Gamma(m_1) \Gamma(m_2)} \left(\frac{z^2 m_1 m_2}{\Omega_1 \Omega_2}\right)^{\frac{m_1+m_2}{2}} K_{(m_1+m_2)}\left(2\sqrt{\frac{z^2 m_1 m_2}{\Omega_1 \Omega_2}}\right) \quad (5)$$

where m_1 and m_2 are the Nakagami parameters of each hop and $K_v(\cdot)$ denotes the modified Bessel Function of second kind with order v [6].

Fig.3. shows a comparison between the density function obtained analytically from (5) with the density function

$$SNR_{V_{sel}} = \frac{1}{\sqrt{N}} \max(Z_1, Z_2) \tag{10}$$

where z_1 and z_2 represents the instantaneous signal voltages at the receiver from two independent diversity paths. For the sake of simplicity and in order to reduce the number of variables the noise power N is assumed to be unity. Therefore (11) may be written as

$$SNR_{V_{sel}} |_{N=1} = \max(Z_1, Z_2) \tag{11}$$

The probability density functions (pdfs) of voltage signal to noise ratio or power signal to noise ratio at the output of the selection combiner are required to evaluate the system performances. In this regard the pdf of the voltage signal to noise ratio is first evaluated by setting the noise power to unity. The other pdf's can be eventually obtained from the above pdf by simple transformation of variables.

The voltage signal to noise ratio at the output of the selection combiner is that of the voltage signal to noise ratio of the strongest diversity branch at its input. For a two branch relay diversity system the output voltage signal to noise ratio is that of branch 1 when the voltage signal to noise ratio of branch 2 is less than or equal to that of branch 1 and vice versa. So if the voltage signal to noise ratio at the output of the selection combiner is denoted by s , it may be concluded that at least one of the diversity branches have the voltage signal to noise ratio equal to s while the others are less than or equal to s .

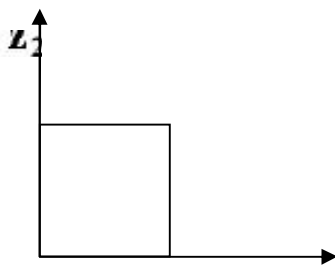


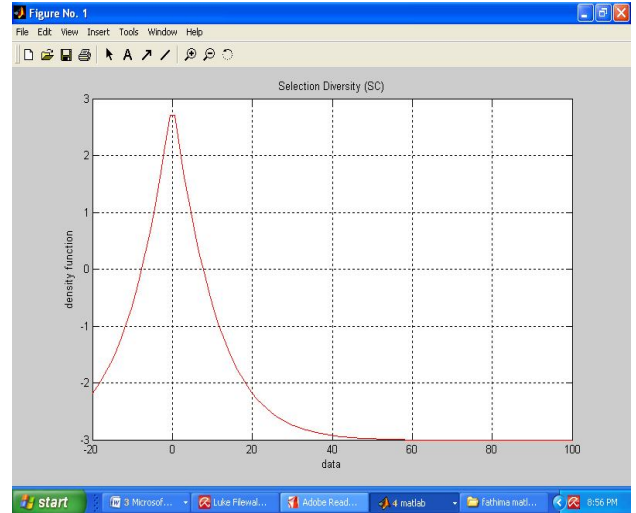
Fig. 6. Combination of values of z_1 and z_2 that forms an envelope s at the output of the selection combiner.

For a two branch diversity system if $z_1 = s$ then $z_2 \leq s$. The line labeled I_1 in Fig. 6. corresponds to this event. The line I_2 corresponds to the situation when $z_1 \leq s$ and $z_2 = s$. The event that the envelope at the output of the selection combiner is s , is the sum of all the events over r_1 and r_2 that produce s as its output. This can be obtained by integrating $f_{Z_1 Z_2}(z_1 z_2)$ along the lines described in Fig. 6. So the envelope at the output of the selection combiner may be written as,

$$f_s(s) = \int_0^s f_{Z_1 Z_2}(Z_1 Z_2) |_{z_1=s} dz_2 + \int_0^s f_{Z_1 Z_2}(Z_1 Z_2) |_{z_2=s} dz_1 \tag{12}$$

$$f_s(s) = I_1 + I_2 \tag{13}$$

$$I_1 = \frac{4}{s\Gamma(m_1)\Gamma(m_2)} \left(\frac{s^2 m_1 m_2}{\Omega_1 \Omega_2} \right)^{\frac{m_1+m_2}{2}} \times K_{(m_1-m_2)} \left(2\sqrt{\frac{s^2 m_1 m_2}{\Omega_1 \Omega_2}} \right) \times \frac{4}{\Gamma(m_3)\Gamma(m_4)} \left(\frac{m_3 m_4}{\Omega_3 \Omega_4} \right)^{\frac{m_3+m_4}{2}} \times \tag{14}$$



$$I_2 = \frac{4}{\Gamma(m_3)\Gamma(m_4)} \left(\frac{s^2 m_3 m_4}{\Omega_3 \Omega_4} \right)^{\frac{m_3+m_4}{2}} \times K_{(m_3-m_4)} \left(2\sqrt{\frac{s^2 m_3 m_4}{\Omega_3 \Omega_4}} \right) \times \int_0^s z_2^{m_3+m_4-1} K_{(m_1-m_2)} \left(2\sqrt{\frac{z_2^2 m_3 m_4}{\Omega_3 \Omega_4}} \right) dz_2 \tag{15}$$

$$\times \frac{4}{\Gamma(m_1)\Gamma(m_2)} \left(\frac{m_1 m_2}{\Omega_1 \Omega_2} \right)^{\frac{m_1+m_2}{2}} \times \int_0^s z_1^{m_1+m_2-1} K_{(m_1-m_2)} \left(2\sqrt{\frac{z_1^2 m_1 m_2}{\Omega_1 \Omega_2}} \right) dz_1$$

In a more compact form the density function at the output of the selection combiner may be written as [7],

$$f_s(s) = C \{ s^{m_1+m_2-1} K_{(m_1-m_2)} \left(2\sqrt{\frac{s^2 m_1 m_2}{\Omega_1 \Omega_2}} \right) \left(\frac{1}{\alpha} \right)^{m_3+m_4} \int_0^{\alpha s} Z^{m_3+m_4-1} K_{(m_3-m_4)}(z) dz \} \tag{16}$$

$$\begin{aligned}
 & + \{ s^{m_3+m_4-1} K_{(m_3-m_4)} \left(2\sqrt{\frac{s^2 m_3 m_4}{\Omega_3 \Omega_4}} \right) \\
 & \left(\frac{1}{\alpha} \right)^{m_1+m_2} \int_0^{\beta s} Z^{m_1+m_2-1} K_{(m_1-m_2)}(t) dt \} \\
 & \text{Where,} \\
 C = & \frac{16}{\prod_{i=1}^4 \Gamma(m_i)} \left(\frac{m_1 m_2}{\Omega_1 \Omega_2} \right)^{\frac{m_1+m_2}{2}} \left(\frac{m_3 m_4}{\Omega_3 \Omega_4} \right)^{\frac{m_3+m_4}{2}} \\
 \alpha = & 2\sqrt{\frac{m_3 m_4}{\Omega_3 \Omega_4}} \quad , \quad \beta = 2\sqrt{\frac{m_1 m_2}{\Omega_1 \Omega_2}}
 \end{aligned}$$

Fig. 7. gives the plot of the density functions at the output of the selection combiner for the equation given in (16) as well for the density function obtained through simulation for the same parameters. The m -parameters of all the four links, of the two branches, were set to unity. $\Omega_1, \Omega_2, \Omega_3$ and Ω_4 were taken to be 2.

Fig. 7. Pdf of the envelope at the output of a selection combiner.

The simulations were done in MATLAB. The Nakagami-m distributed random variables were generated following the procedure given in [8]. Selection at the receiver was done based on the signal strengths.

$f_s(s)$ gives the voltage signal to noise ratio at the output of the selection combiner assuming the noise power to be unity. The power signal to noise ratio is of more relevance and can be obtained from $f_s(s)$ by simple substitution of variables.

The power signal to noise ratio and the voltage signal to noise ratio are related as

$$SNR_{P|N=1} = (SNR_{V|N=1})^2 \quad (17)$$

$$\overline{w} = S^2 \quad (18)$$

The probability density function of w can be obtained from that of s [10]

$$f_w(W) = \frac{1}{2\sqrt{w}} f_s(\sqrt{w}) + \frac{1}{2\sqrt{w}} f_s(-\sqrt{w}) \quad (19)$$

Since the pdf of s exists only for the positive values, hence the second term of (19) is zero.

$$f_w(W) = \frac{1}{2\sqrt{w}} f_s(\sqrt{w}) \quad (20)$$

All the above pdf's have been derived for unity noise power. But the pdf of the power signal to noise ratio for any arbitrary noise power is of theoretical importance and can be derived from (19). If w_N represents the signal to noise ratio for any arbitrary power N ,

$$\overline{w}_N = \frac{\overline{w}}{N} \quad (21)$$

The pdf of w_N is related to that of w by [10]

$$f_{w_N}(\overline{w}_N) = N f_w(N\overline{w}_N) \quad (22)$$

Substituting (20) in (22)

$$f_{w_N}(\overline{w}_N) = \frac{\sqrt{N}}{2\sqrt{\overline{w}_N}} f_s(\sqrt{N\overline{w}_N}) \quad (23)$$

On further simplification,

$$f_{w_N}(\overline{w}_N) = \frac{\sqrt{N}}{2\sqrt{\overline{w}}} f_s(\sqrt{\overline{w}}) \quad (24)$$

Combining (16) and (24) we obtain

$$\begin{aligned}
 f_{w_N}(\overline{w}_N) = & \left\{ \frac{C\sqrt{N}}{2\sqrt{\overline{w}_N}} \right. \\
 & \left(\sqrt{N\overline{w}_N} \right)^{m_1+m_2-1} K_{(m_1-m_2)} \left(2\sqrt{\frac{N\overline{w}_N m_1 m_2}{\Omega_1 \Omega_2}} \right) \\
 & \alpha \int_0^{\sqrt{N\overline{w}_N}} t^{m_3+m_4-1} K_{(m_3-m_4)}(t) dt \} + \left\{ \left(\sqrt{N\overline{w}_N} \right)^{m_3+m_4-1} \right. \\
 & K_{(m_3-m_4)} \left(2\sqrt{\frac{N\overline{w}_N m_3 m_4}{\Omega_3 \Omega_4}} \right) \left(\frac{1}{\beta} \right)^{m_1+m_2} \int_0^{\beta \sqrt{N\overline{w}_N}} t^{m_1+m_2-1} \\
 & K_{(m_1-m_2)}(t) dt \} \quad (25)
 \end{aligned}$$

For $m_1=m_2=m_3=m_4=1$ and $\Omega_1=\Omega_2=\Omega_3=\Omega_4=2$, the power signal to noise ratio at the output of the selection combiner may be written as,

$$\begin{aligned}
 f_{w_N}(\overline{w}_N) = & \frac{\sqrt{N}}{2\sqrt{\overline{w}_N}} \left\{ \left(\sqrt{N\overline{w}_N} \right) K_0 \left(\sqrt{N\overline{w}_N} \right) \int_0^{\sqrt{N\overline{w}_N}} t K_0(t) dt \right\} \\
 & + \left\{ \left(\sqrt{N\overline{w}_N} \right) K_0 \left(\sqrt{N\overline{w}_N} \right) \int_0^{\sqrt{N\overline{w}_N}} t K_0(t) dt \right\} \quad (26)
 \end{aligned}$$

B. Maximal Ratio Combining

In this section, the probability density function of the SNR at the output of a maximal ratio combiner at the destination node of Fig. 4. is evaluated. The individual links are assumed to be Nakagami faded as earlier. The density functions for both voltage signal to noise and power signal to noise ratio are derived. The voltage signal to noise ratio and power signal to noise ratio are denoted as SNR_{VMRC} and SNR_{PMRC} respectively. The two signal to noise ratios are related to each other and to the input signals of the two diversity branches

$$SNR_{VMRC} = \sqrt{SNR_{PMRC}} = \frac{1}{\sqrt{N}} \sqrt{z_1^2 + z_2^2} \quad (27)$$

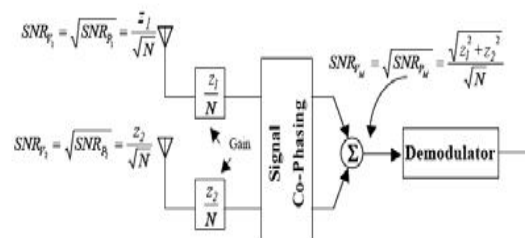


Fig. 8. Block

diagram of a two-branch maximal ratio combiner having equal noise power in both the branches.

The joint probability density function of two independent relay channels is as given in (9). It needs to be integrated to find the probability density function at the output of the maximal ratio combiner. But in Cartesian coordinates the integral becomes very involved. Changing into polar coordinates makes the computations easily tractable. The variables and are written as,

$$Z_1 = m \cos \phi \tag{28}$$

$$Z_2 = m \sin \phi \tag{29}$$

as, $z_1 \geq 0$ and $z_2 \geq 0$, so $0 \leq \phi \leq \pi/2$. The new probability density function can be deduced from (9), by change of variables and introduction of the Jacobian of the transformation. The new density function is defined as,

$$f_{M\Phi}(m, \phi) = |\tilde{J}| \cdot f_{Z_1 Z_2}(z_1, z_2) \tag{30}$$

where J represents the Jacobian.

$$\tilde{J} = \begin{vmatrix} \frac{\partial z_1}{\partial m} & \frac{\partial z_1}{\partial \phi} \\ \frac{\partial z_2}{\partial m} & \frac{\partial z_2}{\partial \phi} \end{vmatrix} \tag{31}$$

Therefore, (5.28) gets modified to,

$$f_{M\Phi}(m, \phi) = m \cdot f_{Z_1 Z_2}(z_1, z_2) \Big|_{\substack{z_1 = m \cos \phi \\ z_2 = m \sin \phi}} \tag{32}$$

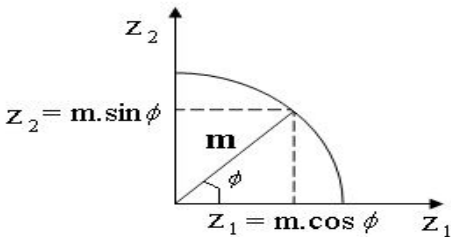


Fig. 9.

Combination of values of z_1 and z_2 that forms an envelope m at the output of the maximal ratio combiner.

In (31) ϕ varies from 0 to $\pi/2$. So, $f_M(m)$ may be written as,

$$f_M(m) = \int_0^{\pi/2} f_{M\Phi}(m, \phi) d\phi \tag{33}$$

Substituting (31) into (32),

$$f_M(m) = C m^{m_1+m_2+m_3+m_4-1} \times \int_0^{\pi/2} \frac{1}{\sin \phi \cos \phi} \cos^{m_1+m_2}(\phi) \sin^{m_3+m_4}(\phi) d\phi$$

$$K_{(m_1-m_2)} \left(2 \sqrt{\frac{m^2 \cos^2(\phi) m_1 m_2}{\Omega_1 \Omega_2}} \right) \times K_{(m_3-m_4)} \left(2 \sqrt{\frac{m^2 \sin^2(\phi) m_3 m_4}{\Omega_3 \Omega_4}} \right) d\phi \tag{34}$$

Where,

$$C = \frac{16}{\prod_{i=1}^4 \Gamma(m_i)} \left(\frac{m_1 m_2}{\Omega_1 \Omega_2} \right)^{\frac{m_1+m_2}{2}} \left(\frac{m_3 m_4}{\Omega_3 \Omega_4} \right)^{\frac{m_3+m_4}{2}}$$

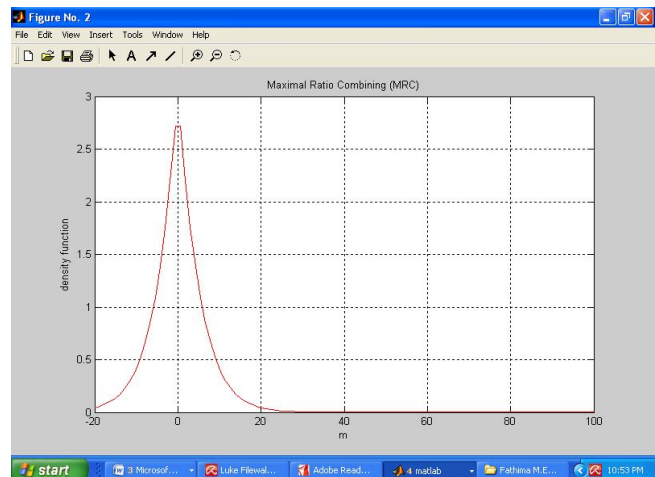
The density function at the output of the MRC given by (34) requires to be evaluated numerically for specific values of m_i and Ω_i , where $i=1,2,\dots,4$.

For specific case when $m_i=1$ and $\Omega_i = 2$ for $i = 1,\dots,4$. (33) reduces to [11]

$$f_M(m) = C m^3 \cdot \int_0^{\pi/2} \cos(\phi) \cdot \sin(\phi) \cdot K_0(m \cos(\phi)) \cdot K_0(m \sin(\phi)) d\phi \tag{36}$$

The above integral has been computed numerically to obtain the final density function at the output of maximal ratio combiner as shown in Fig (10).

Fig. 10. Pdf of the envelope at the output of the maximal ratio combiner.



IV. BER PERFORMANCE

In Fig. 11. the bit error rate performances for selection and maximal ratio combining in the above mentioned cooperative diversity scheme has been plotted. The simulations were carried out by generating random variables having the density functions given by (16) and (35). The random variables were generated by the method of rejection [12].

Fig. 12. plots the bit error rate for the system described in Fig. 4. and having selection combining at the output. The BER obtained for the channel described in eqn. (16) is same as the BER obtained through simulation of the individual

channels, generated according to the methods described in [8], and performing selection combining at the output. The plot in Fig. 12 validates the mathematical derivations. The same were performed for maximal ratio combining at the output and the results were found to be satisfactory.

As mentioned earlier, while evaluating the analytical expressions for the pdf of the two hop relay link, the relay node was assumed to be noise free. Such an assumption of an ideal relay

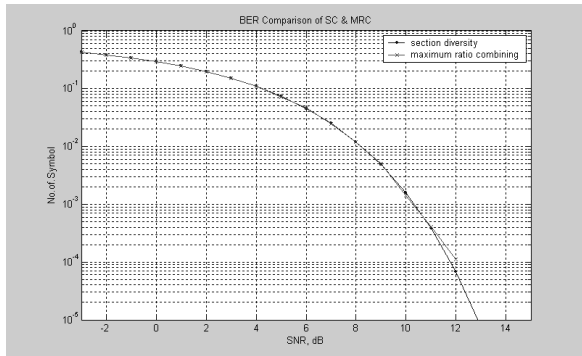
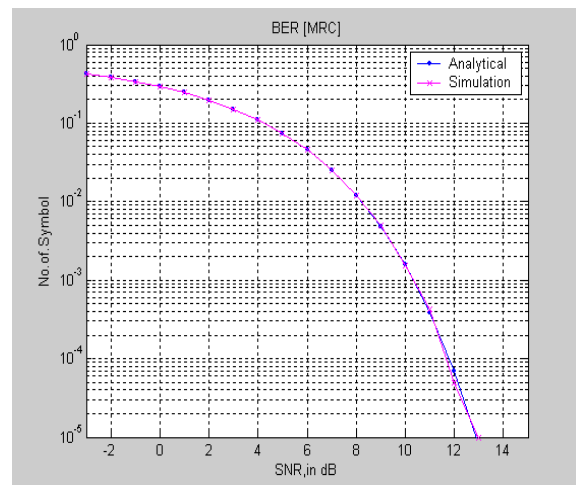


Fig. 11. Plot of bit error rate

Fig. 12. Comparison of bit error rate obtained analytically and from simulation was made to reduce the mathematical complexity in derivation of the pdf expression. In practice the SNR at the relay, what so ever large, will be a finite quantity. It is therefore necessary to estimate the error introduced in computation of BER using the pdf in (5) and find some lower limit on the relay SNR above which the error in BER will be reasonably small. To study the behavior of error in link BER as a function of SNR at the relay, we have computed the BER Vs SNR at the destination node with SNR at the relay as a parameter. The range of destination SNR has been taken as 0 - 30dB and the same range has been used for the relay SNR as well. From the knowledge of BER values at different destination SNR for a given SNR at the relay and comparing the same with the BER values those destination SNR's for an ideal relay; we have computed the root mean square (RMS) error in BER at the given relay SNR.

V. CONCLUSION.

In this communication we present the closed form expression for the probability density function of the signal envelope at the output of a selection combiner and maximal ratio combiner, having signals from two independent relay channels as inputs. The channel statistics of the individual hops of a relay diversity branch were assumed to be Nakagami-m distributed. We also evaluate the end-to-end density function of a two hop relay branch, with each hop being Nakagami-m distributed. The analytical results were verified through simulation for particular cases. The bit error rates for the two combining schemes (selection combining and maximal ratio combining) were also evaluated for the system shown in Fig.4.



REFERENCES

- [1] A. Sendonaris, E. Erkip, and B. Aazhang, "User cooperation diversity part- I: system description," *IEEE Transactions on Communications*, vol.51, no. 11, November 2003.
- [2] A. Sendonaris, E. Erkip, and B. Aazhang, "User cooperation diversity part- II: implementation aspects and performance analysis," *IEEE Transactions on Communications*, vol. 51, no. 11, November 2003.
- [3] C. S. Patel, G. L. Stuber, T. G. Pratt, "Statistical properties of amplify and forward relay fading channels," *IEEE Transactions on Vehicular Technology*, vol. 55, no. 1, January 2006.
- [4] M. Nakagami, "The m-distribution-a general formula of intensity distribution of rapid fading," in *Statistical Methods in Radio Wave Propagation*. Oxford, U.K.: Pergamon, 1960, pp. 3-36.
- [5] G.K. Karagiannidis, N.C. Sagias, and P.T. Mathiopoulos, "The N* Nakagami fading channel model," *2nd International Symposium on Wireless Communication Systems*, September 2005.
- [6] I.S.Gradsteyn and I.M.Ryzhik, *Tables of Integrals, Series, and Products*, 5thed., San Diego, CA: Academic, 1994.
- [7] B. S. Paul and R. Bhattacharjee, "Selection combining of two amplify forward relay branches with individual links experiencing Nakagami fading," *2007 Asia Pacific Conference on Communication*, Oct. 2007.
- [8] N. C. Beaulieu, "Efficient Nakagami-m fading channel simulation," *IEEE Transactions on Vehicular Technology*, vol. 54, no. 2, March 2005.
- [9] W. C. Jakes, *Microwave Mobile Communications*, IEEE Press, 1974.
- [10] V. K. Rohatgi and A. K. Md. Ehsanes Saleh, *An Introduction to Probability and Statistics*. John Wiley & Sons, INC.
- [11] B. S. Paul and R. Bhattacharjee, "Maximal ratio combining of two amplify-forward relay branches with individual links experiencing Nakagami fading," *IEEE TENCON*, Oct.-Nov. 2007.
- [12] W.H. Tranter, K. S. Shanmugan, T. S. Rappaport and K.L.Kosbar, *Principles of Communication Systems Simulation with Wireless Applications*, Prentice Hall, Upper Saddle River, New Jersey.
- [13] Babu Sena Paul and Ratnajit Bhattacharjee, "Analysis of different combining schemes of two amplify forward relay branches with individual links experiencing Nakagami fading" *IEEE Journal on International Journal of Information Technology*, Vol no.4 ,no.27.